

Data Assimilation Experiments using CHAMP Refractivity Data

Hiromu SEKO¹, Yoshinori SHOJI¹, Masaru KUNII¹, Kazuo SAITO¹, Yuichi AOYAMA²

¹ Meteorological Research Institute, Japan Meteorological Agency, Tsukuba, Japan

² National Institute of Polar Research

1. Introduction Heavy rainfalls occur when a large amount of water vapor was supplied to rainfall systems. Middle-level dry air also enhances the convections due to the destabilizing of the convective stability. Because water vapor is one of important factors that control rainfall, the water vapor data is expected to improve the rainfall prediction when it is assimilated into the initial condition of numerical models. In this study, the vertical refractivity profile at the tangent point, which is the closest point on the path from GPS satellite and CHAMP, was used as assimilation data. However, there are two problems in the assimilation. (1) The resolution of refractivity data provided by GFZ is 200m. Generally, the data is thinned out to reduce the correlation of the observation error. However, the thinned data became the impact of data assimilation weaker. (2) Actual observed value is the integrated value along the path, because the CHAMP receives the signal that penetrated through the atmosphere. The tangent point value is estimated by using the assumption the refractivity is uniform in the horizontal direction. However, the refractivity does not always satisfy this assumption. Thus, the assimilation method of the high-resolution path-refractivity data should be developed.

2. Numerical model and refractivity data observed by CHAMP In this study, the refractivity data was assimilated into the Meso Spectrum Model (MSM) of Japan Meteorological Agency by using the Meso-4DVar Data Assimilation System (Koizumi et al., 2005). Firstly, the bias and RMSE of D-value, which is difference of observation and first guess value, was investigated by using the data of July 2004. Because the large bias existed below 2km, the data above the 2km was used in this study. The observation error of the tangent point data was also estimated from RMSE. Figure 1 shows the impact of the tangent point data. The small observation error was given to show the impact more clearly. When the CHAMP data was assimilated, the precipitation region became close to the observed one. This, the CHAMP data has the potential to improve the rainfall forecast. When the thinning was performed, the precipitation was not reproduced (not shown).

3. Vertical correlation of observation error The vertical correction of the observation error was estimated by following Chen et al. (2005). They assumed that D-value is sum of the deviations of forecast error and observation error. The deviation of the forecast error was estimated by NMC method (Parrish and Derber, 1992). The correlation coefficient was obtained from the deviation of observation error (fig. 2a), and then the correlation coefficient was simplified (fig. 2b). The observation error covariance was calculated by multiplying the observation error (fig. 2c). The observation error multiplied by 0.1 was used in the following experiments. When observation error covariance was used in the assimilation, the precipitation region was reproduced where they were observed (fig.3a). On the other hand, the precipitation was not reproduced when the vertical correlation was considered (fig. 3b).

4. Assimilation of path-refractivity data Figure 4 shows the schematic illustration of the path data. In the CASE 2, the path-averaged refractivity was assimilated. The path-averaged value was reproduced by the weighted average of the tangent point refractivity data. The weight is the path length within the layer of 200m. The observation error was also estimated by the same way from the observation error of tangent points. The modeled refractivity average was estimated by following procedures; (1) the path was divided into small elements. (2) refractivity at the center of elements was estimated from the grid point values. (3) the value of refractivity multiplied by the element length was added up and then divided by the path length. When the path-averaged value was assimilated, the impact of CHAMP data became smaller (fig. 5). It is deduced that the information of low level humid air was not used to moisten only the lower air in CASE2.

The vertical correlation of the path data is also considered in the same way as the tangent point. When the path-averaged refractivity was assimilated with consideration of the vertical correlation of observation error, the precipitation became stronger and became closer to the observed one (fig. 6).

Acknowledgments

CHAMP data were provided from GFZ. The initial and boundary conditions of MSM were provided from the Numerical Prediction Division (NPD) of JMA. We also used MSM and Meso-4DVar system developed by NPD/JMA. We would like to thank Dr. Wickert of GFZ and members of NPD/JMA.

References

- Chen, S.-Y., Y.-H. Kuo, S. Sokolovskiy and C.-Y. Huang, 2005: Estimation of observational errors of GPS radio occultation soundings. Second GPS RO Data Users Workshop, 22-24 August 2005, Lansdowne, USA.
- Parrish, D.F. and J.C. Derber, 1992: The national meteorological center's spectral statistical-interpolation analysis system. *Mon. Wea. Rev.*, **120**, 1747-1763.

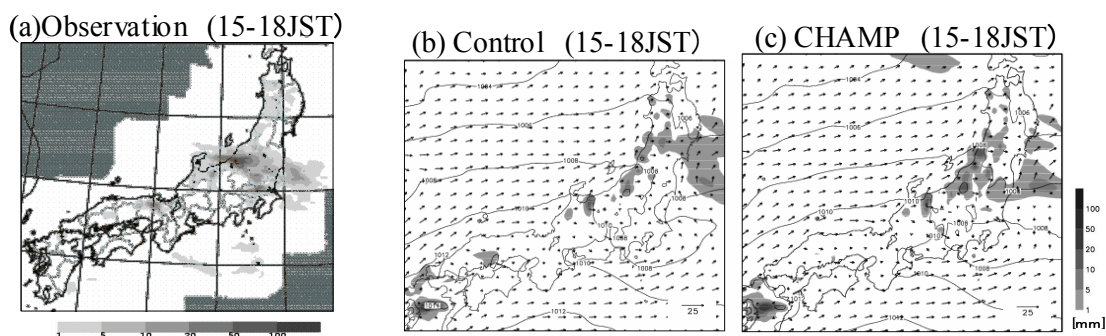


Fig.1 (a) Precipitation region observed by the convective radars from 15JST to 18JST on 16 July 2004. Shaded region in (b) and (c) indicate the precipitation region predicted by Meso-scale model from the analyzed fields. Analyzed fields were obtained by the assimilation of (b) conventional data and of (c) conventional data and CHAMP data

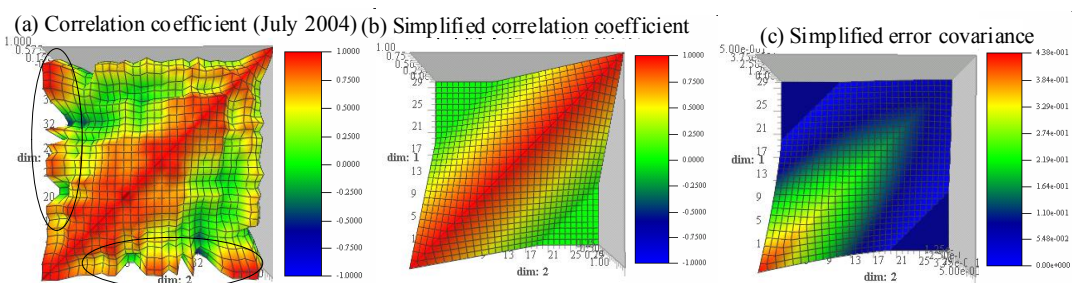


Fig. 2 (a) Vertical correlation of observation data, (b) simplified correlation and (c) observation error covariance. Observation error was estimated from the D-value of July 2004

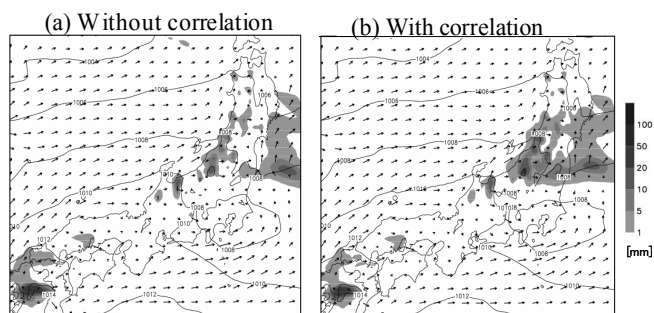


Fig. 3 Precipitation region predicted from the analyzed fields. Analyzed fields was obtained by the assimilation of refractivity data (a) without and (b) with consideration of the vertical correlation of the observation data.

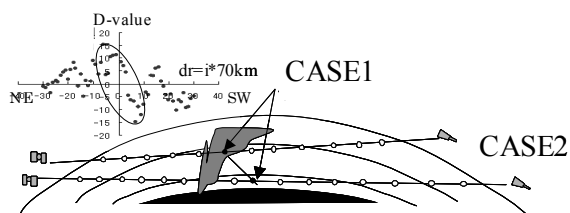


Fig. 4 Schematic illustration of positions of the assimilation data and (upper right) distribution of D-values along the observed path.

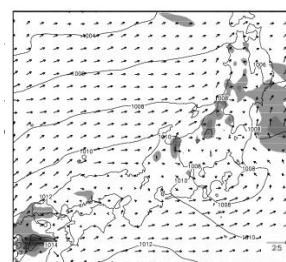


Fig. 5 Precipitation regions predicted from the analyzed fields. The analyzed fields were obtained by assimilation of CASE2.

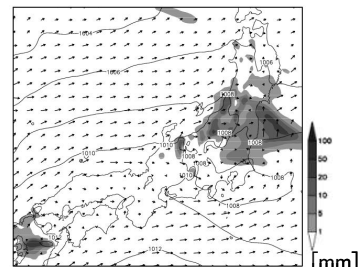


Fig. 6 Precipitation regions predicted from the analyzed fields. The analyzed fields were obtained by assimilation of CASE2 with the consideration of the vertical correlation of the observed data .